Kinetic undercooling in Hele-Shaw flows

Pedro H. A. Anjos, Eduardo O. Dias,* and José A. Miranda†
Departamento de Física, Universidade Federal de Pernambuco, Recife, Pernambuco 50670-901, Brazil
(Received 27 August 2015; published 26 October 2015)

A central topic in Hele-Shaw flow research is the inclusion of physical effects on the interface between fluids. In this context, the addition of surface tension restrains the emergence of high interfacial curvatures, while consideration of kinetic undercooling effects inhibits the occurrence of high interfacial velocities. By connecting kinetic undercooling to the action of the dynamic contact angle, we show in a quantitative manner that the kinetic undercooling contribution varies as a linear function of the normal velocity at the interface. A perturbative weakly nonlinear analysis is employed to extract valuable information about the influence of kinetic undercooling on the shape of the emerging fingered structures. Under radial Hele-Shaw flow, it is found that kinetic undercooling delays, but does not suppress, the development of finger tip-broadening and finger tip-splitting phenomena. In addition, our results indicate that kinetic undercooling plays a key role in determining the appearance of tip splitting in rectangular Hele-Shaw geometry.

DOI: 10.1103/PhysRevE.92.043019 PACS number(s): 47.15.gp, 47.20.Ma, 47.54.−r, 68.70.+w

I. INTRODUCTION

The Saffman-Taylor instability [1] is one of the most studied problems among fluid dynamic systems presenting the formation and evolution of patterned structures [2]. This instability arises when a fluid displaces another of higher viscosity in the narrow gap separating two flat, parallel glass plates of a Hele-Shaw cell. The lower viscosity fluid penetrates the more viscous one, leading to the development of an interfacial pattern resembling a set of fingerlike structures. This characterizes a phenomenon commonly known as viscous fingering that is governed by a dynamic competition process between surface tension and viscous forces or pressure gradients.

For longitudinal flow in a rectangular channel (rectangular Hele-Shaw cell) [3–8], typically the system evolves until a single stable finger is formed. On the other hand, for radial fluid injection (radial Hele-Shaw cell) [9–14], the fingers tend to split at their tips and evolve into a complex branched morphology. In contrast to the radial flow case, displacements in rectangular geometry normally display no tip-splitting events. Nevertheless, numerical simulations [3,15,16] and experiments [6,17,18] for rectangular geometry flow indicate that fingers may undergo a tip-splitting instability, but in the late stages of interface evolution and if the speed of flow is sufficiently high. In this setting, one can say that finger tip splitting is a basic mechanism of the viscous fingering process.

The dynamic evolution of the Saffman-Taylor problem is governed by the Hele-Shaw flow equations, described by a quasi-two-dimensional, gap-averaged Darcy's law (essentially, fluid velocity proportional to the negative of the pressure gradient) and fluid incompressibility (divergenceless velocity field). These fundamental equations are supplemented by two boundary conditions at the fluid-fluid interface [1–5,9,14]: a pressure jump, as given by a Young-Laplace equation, and the continuity (kinematic) condition for the normal component of the fluid velocity. The pressure jump equation is particularly important since it considers the competition between destabilizing and stabilizing effects acting at the two-fluid interface. Stabilizing (or regularizing) effects can be incorporated into the Hele-Shaw moving boundary problem by adding extra terms into the Young-Laplace boundary condition. For instance, the inclusion of a term involving the product of surface tension σ by the interfacial curvature κ penalizes large curvatures and prevents the formation of unphysical cusp singularities on the interface [15,19–21].

An alternative regularizing strategy considers the addition of a different extra term into the Young-Laplace condition, which disfavors the emergence of large normal velocities at the interface. This regularization procedure is known as kinetic undercooling and involves the product cv_n, where c is the kinetic undercooling parameter and v_n is the normal velocity at the interface. It is worth noting that such a kinetic undercooling regularizing approach has been largely used in the study of melting and freezing, Stefan-type problems [22–25], and in particular for investigations of interfacial instabilities and pattern formation of growing dendrites [23,26,27]. It has also been utilized in the research of finger-shaped electrical discharges, known as streamers [28,29].

Interestingly, the study of the Saffman-Taylor problem with kinetic undercooling has been considerably unappreciated compared to those equivalent studies that take into account the stabilizing or regularizing role of surface tension [2,15,19–21]. In the framework of Hele-Shaw flows, a kinetic undercooling-type condition was considered some time ago by Romero [30], who carried out a theoretical study that incorporated, in an *ad hoc* manner, a contribution linearly proportional to v_n into the Young-Laplace pressure boundary condition. In Ref. [30], it was assumed that this kinetic undercooling term was connected to the interfacial curvature along the transverse direction to Hele-Shaw cell plates. Unfortunately, no quantitative justification for this particular assumption was given in [30]. Then, in the early 1990s, Weinstein *et al.* [31] addressed this issue and incorporated a dynamic contact angle model for viscous fingering in a rectangular Hele-Shaw cell. However, as pointed out in Ref. [32], the asymptotic analysis implemented by Weinstein *et al.* relies on a steady state assumption, so that it is not directly applicable to the

*eduardodias@df.ufpe.br
†jme@df.ufpe.br

more general radial Hele-Shaw flow problem, in which the two-fluid interface varies with time.

Despite the *ad hoc* nature of the kinetic undercooling contribution proposed in Ref. [30] and the still incomplete approach proposed in Ref. [31], very recently Dallaston and co-workers revisited the problem and analyzed the effects of surface tension and kinetic undercooling in both rectangular and radial Hele-Shaw cell setups [33–36]. A number of interesting results were found. For example, their analytical linear stability study of the radial flow geometry [33] showed that in contrast to the injection situation (expansion of a less viscous bubble) where surface tension and kinetic undercooling are both stabilizing, under suction (contraction of a less viscous bubble) these two effects act in opposition (i.e., surface tension stabilizes the boundary, while kinetic undercooling destabilizes it).

In Ref. [34], Dallaston and McCue performed numerical simulations for bubble expansion and contraction during the advanced time regime. It was found that kinetic undercooling tends to delay the formation of fingers during expansion, while it favors the occurrence of bubble pinch-off during contraction. Stability analysis, i.e., numerical and exact solution techniques for the radial and rectangular geometries, were employed in Ref. [35], where it was verified that fingers form for lower kinetic undercooling, and that corners arise for sufficiently high kinetic undercooling values. Finally, in Ref. [36], these investigators focused on the study of finger formation and finger selection in rectangular flow circumstances, where it was demonstrated that kinetic undercooling acts against the establishment of high velocities and prevents blow-up of unregularized solutions.

Two main reasons motivated us to pursue the research presented in this work: first is the *ad hoc* assumption [30] that for Hele-Shaw flows, the kinetic undercooling term takes the specific functional form cv_n (a linear function of the normal interface velocity). Notice that in Refs. [30,33–36], not much has been said about the physical nature of the undercooling parameter c and its relation to other important physical quantities of the problem. These issues still need to be examined. The second motivation comes from the suggestive results obtained in Refs. [33–36] which used linear stability analysis and numerical simulations to study the role played by kinetic undercooling during early and advanced time regimes, respectively. So, an investigation about the intermediate stage of the system's pattern-forming dynamics that bridges early linear and fully nonlinear regimes is still lacking.

In this work, first we show that the assumed connection between the dynamic contact angle and the normal interface velocity can be derived in a quantitative fashion with the help of the so-called Hoffman-Voinov-Tanner law [37–42]. Then, we focus our attention on the intermediate dynamic regime, in which nonlinear effects start to play a role in determining the most relevant morphological features of the fluid-fluid interface. We do this by employing a weakly nonlinear analysis of the problem [7,14] and examine the influence of the kinetic undercooling term on the shape of the emerging fingering patterns, mainly on its impact on finger tip-broadening and finger tip-splitting events. In this framing, our weakly nonlinear approach allows one to gain valuable analytical insights into the effects of the dynamic contact angle on the development of the Saffman-Taylor instability in both radial and rectangular Hele-Shaw geometries.

II. PHYSICAL PROBLEM AND GOVERNING EQUATIONS

In this section, we describe the injection-driven Saffman-Taylor problem in a radial Hele-Shaw cell and introduce the related governing equations. In Sec. II A, we provide a quantitative derivation of the Young-Laplace pressure jump boundary condition which considers the inclusion of dynamic contact angle effects. This consideration plus the use of the Hoffman-Voinov-Tanner law leads to a kinetic undercooling contribution that is indeed a linear function of the normal velocity on the interface [Eqs. (9) and (10)].

Section II B is devoted to the derivation of a second-order mode-coupling differential equation that allows one to describe the time evolution of the interfacial perturbation amplitudes [Eqs. (11)–(15)]. This nonlinear differential equation permits the analytical investigation of the impact of kinetic undercooling on the dynamical evolution and on the main morphological features of the viscous fingering patterns. The influence of kinetic undercooling on the fingering instability in the radial (rectangular) Hele-Shaw cell setup will be discussed in Sec. III A (Sec. III B).

A. Physical origin of kinetic undercooling in Hele-Shaw flows

We start by describing the physical system of interest. Consider a Hele-Shaw cell of gap spacing b, in which a fluid of viscosity η_2 is displaced by the radial injection of a less viscous fluid of viscosity η_1. The fluids are immiscible and incompressible, and fluid 1 is injected at the center of the cell at a constant injection rate Q (equal to area covered per unit time). Between the two fluids, there exists a surface tension σ. We focus on the most unstable Saffman-Taylor situation in which $\eta_2 \gg \eta_1$, so that the viscosity contrast $A = (\eta_2 - \eta_1)/(\eta_1 + \eta_2) \approx 1$.

The governing equations of the effectively two-dimensional radial Hele-Shaw cell problem are the gap-averaged Darcy's law [1,2,9],

$$\mathbf{v}_j = -\frac{b^2}{12\eta_j}\nabla p_j, \tag{1}$$

and the gap-averaged incompressibility condition,

$$\nabla.\mathbf{v}_j = 0, \tag{2}$$

where $\mathbf{v}_j = \mathbf{v}_j(r,\varphi)$ and $p_j = p_j(r,\varphi)$ are the velocity and pressure of fluid j, respectively, with $j = 1,2$. The radial coordinate r denotes the distance to the injection source point, which is chosen as the origin of the polar coordinate system. In addition, the polar angle is denoted by φ.

The irrotational nature of the flow ($\nabla \times \mathbf{v}_j = 0$) allows one to define a velocity potential that obeys the Laplace equation $\nabla^2\phi_j = 0$. In order to describe the dynamics of the evolving interface, we have to relate the velocity potential $\phi_j(r,\varphi)$ to the position of the interface $\mathcal{R}(\varphi,t)$. This can be accomplished by using the kinematic boundary condition,

$$\frac{\partial \mathcal{R}}{\partial t} = \left(\frac{1}{r^2}\frac{\partial \mathcal{R}}{\partial \varphi}\frac{\partial \phi_j}{\partial \varphi}\right)_{r=\mathcal{R}} - \left(\frac{\partial \phi_j}{\partial r}\right)_{r=\mathcal{R}}, \tag{3}$$

which states that the normal components of each fluid velocity are continuous at the interface.

The problem is then entirely specified by the pressure boundary condition that is expressed by the celebrated Young-Laplace condition [1–14]. This relation considers a pressure jump at the interface $\Delta p = (p_1 - p_2)|_{\mathcal{R}}$, given by

$$\Delta p = \sigma\kappa - \frac{2\sigma}{b}\cos\theta_s. \tag{4}$$

The first term on the right-hand side represents the contribution of the surface tension coming from the interfacial curvature on the plane of the Hele-Shaw cell. On the other hand, the second term on the right-hand side of (4) refers to the effect of the curvature associated with the interface profile in the direction perpendicular to the Hele-Shaw cell plates. Here, θ_s is the static contact angle measured between the plates and the curved meniscus [assumed to be circular with radius $b/(2\cos\theta_s)$].

In fact, Eq. (4) represents the simplest and most traditional way [1–14] to model the pressure jump in the development of the Saffman-Taylor instability. However, most previous studies largely neglect the important hydrodynamic effects related to the moving contact line. The moving contact line consists of the contact region of the two fluids with the glass plate (i.e., a three-phase line moving in relation to a solid substrate). This phenomenon yields to a local dynamic contact angle θ_d that depends on the local velocity U at which the contact line moves over the solid plates. In this paper, we are interested to go one step further and study the impact of θ_d on the viscous fingering instability. So, we use Eq. (4) as a starting point and from it try to add, also in a simple way, the effects related to the dynamic contact angle.

We begin by considering a velocity dependent expression for θ_d that is quantified by the classical Hoffman-Voinov-Tanner law [37–43],

$$\theta_d^3 = \theta_s^3 + \ell\mathrm{Ca}, \tag{5}$$

where $\mathrm{Ca} = \eta_2 U/\sigma$ is the capillary number that measures the ratio between viscous and surface tension forces, and $\theta_d < 3\pi/4$. In addition, $\ell = 9\ln(Y/Y_\infty)$, where Y is a macroscopic scale related to the gap thickness b, and Y_∞ represents a microscopic cutoff length scale where macroscopic hydrodynamic models break down [43]. As evaluated in Refs. [37,41,43], by setting $Y \approx b$, one gets $\ell \approx 80 - 100$. As discussed in detail in Refs. [37–43], it should be pointed out that Eq. (5) holds if the following simplifying assumptions are applied: (i) the capillary number is small ($\mathrm{Ca} \lesssim 0.1$); (ii) inertial effects can be neglected; and (iii) the surfaces are perfect (no heterogeneity), so that there is no contact angle hysteresis. All of these conditions hold for our current Hele-Shaw cell problem.

By assuming small capillary numbers in (5) and considering the leading kinetic correction from the dynamic contact angle, we obtain

$$\theta_d = \theta_s\left(1 + \frac{\ell\mathrm{Ca}}{3\theta_s^3}\right). \tag{6}$$

The influence of the dynamic contact angle on the pressure discontinuity can be accessed by replacing θ_s in Eq. (4) with θ_d as defined by Eq. (6). Making this substitution and expanding $\cos[\theta_s + \ell\mathrm{Ca}/(3\theta_s^2)]$ in the Young-Laplace expression (4) results in

$$\Delta p = \sigma\kappa - \frac{2\sigma}{b}\left[\cos\theta_s\cos\left(\frac{\ell\mathrm{Ca}}{3\theta_s^2}\right) - \sin\theta_s\sin\left(\frac{\ell\mathrm{Ca}}{3\theta_s^2}\right)\right], \tag{7}$$

where by assuming that $\mathrm{Ca} \ll 1$, we get

$$\Delta p \approx \sigma\kappa - \frac{2\sigma}{b}\left[\cos\theta_s - \sin\theta_s\left(\frac{\ell\mathrm{Ca}}{3\theta_s^2}\right)\right]. \tag{8}$$

By inspecting Eq. (8), one readily notices that the contribution of the dynamic contact angle naturally implies a linear dependence on the interface velocity, when the small capillary number limit is considered. It is worth noting that this result is in line with that obtained in Ref. [44] for immiscible fluid displacements in capillary tubes.

To complete the description of the governing equations for the radial Hele-Shaw flow when dynamic contact angle effects are taken into account, we consider the speed of moving contact line U as given by the normal velocity of the interface v_n, and conveniently rewrite Eq. (8) as

$$\Delta p = \sigma\kappa - \frac{2\sigma}{b}\cos\theta_s + cv_n, \tag{9}$$

where

$$c = \frac{2\ell\eta_2\sin\theta_s}{3b\theta_s^2}. \tag{10}$$

Equation (9) is one of the central results of our current work. It clearly indicates the physical connection between the kinetic undercooling effect (quantified by the term cv_n) and the action of the dynamic contact angle. Recall that as emphatically pointed out in Sec. I, such a connection has been incorporated in an *ad hoc* manner in most previous works on this topic. In addition, from Eq. (10), one can readily see that the kinetic undercooling parameter c is now explicitly written in terms of the static contact angle θ_s, viscosity of the displaced fluid η_2, gap thickness b, and microscopic length scales of the flow incorporated in ℓ.

Before we advance, it should be noted that the influence of the dynamic contact angle on viscous fingering patterns has also been analyzed in Ref. [43]. However, this has been done in a different context. In [43], the instability dynamics takes place in a rotating Hele-Shaw cell, where a completely wetting fluid is assumed to be confined between the glass plate. As discussed in [43], under such circumstances, the static contact angle could be safely neglected ($\theta_s \approx 0$), and consequently the action of the dynamic contact angle on the pressure jump condition was given by a term proportional to $\mathrm{Ca}^{2/3}$. Therefore, in this case, the linear dependence of the pressure jump condition on the normal velocity of the interface as expressed by Eq. (9) is not verified.

B. Mode-coupling differential equation including kinetic undercooling

At this point, we have all of the ingredients to obtain the second-order, mode-coupling differential equation for the fluid interface evolution when kinetic undercooling effects are taken into consideration. Within our perturbative approach, we can represent the expanding two-fluid interface as

$\mathcal{R}(\varphi,t) = R(t) + \zeta(\varphi,t)$, where $R(t) = (R_0^2 + Qt/\pi)^{1/2}$ is the time-dependent unperturbed radius, with R_0 being the unperturbed radius at $t = 0$. Here, $\zeta(\varphi,t) = \sum_{n=-\infty}^{+\infty} \zeta_n(t) \exp(in\varphi)$ is the net interface perturbation with Fourier amplitudes $\zeta_n(t)$ and integer wave numbers n. Our current weakly nonlinear analysis keeps terms up to the second order in ζ and uses mass conservation to connect the zeroth mode amplitude to the other modes as $\zeta_0 = -(1/2R)\sum_{n\neq 0} |\zeta_n(t)|^2$.

Following standard steps performed in weakly nonlinear studies of Hele-Shaw flows [7,14], we evaluate the velocity potential at the fluid interface and use the kinematic boundary condition (3) to express ϕ in terms of ζ_n. By substituting the result of this calculation and the pressure boundary condition (9) into Darcy's law (1), always keeping terms up to second order in ζ, and then Fourier transforming, we obtain the equation of motion for the perturbation amplitudes (for $n \neq 0$),

$$\dot{\zeta}_n = \lambda(n)\zeta_n + \sum_{n'\neq 0}[F(n,n')\zeta_{n'}\zeta_{n-n'} + G(n,n')\dot{\zeta}_{n'}\zeta_{n-n'}], \quad (11)$$

where the overdot denotes the total time derivative,

$$\lambda(n) = \frac{1}{1+\Theta(n)}\left\{\frac{Q(|n|-1)}{2\pi R(t)^2} - \frac{\alpha|n|(n^2-1)}{R(t)^3}\right\} \quad (12)$$

is the linear growth rate, $\alpha = b^2\sigma/(12\eta_2)$, and the function

$$\Theta(n) = \frac{cb^2|n|}{12\eta_2 R(t)} \quad (13)$$

accounts for the action of the kinetic undercooling effect.

The second-order mode-coupling terms are given by

$$F(n,n') = \frac{1}{1+\Theta(n)}\left\{\frac{Q|n|}{2\pi R(t)^3}\left[\frac{1}{2} - \mathrm{sgn}(nn')\right] - \frac{\alpha|n|}{R(t)^4}\left[1 - \frac{n'}{2}(3n'+n)\right] - \Theta(n)\frac{Q}{4\pi R(t)^3}n'(n-n')\right\} \quad (14)$$

and

$$G(n,n') = \frac{1}{1+\Theta(n)}\left\{\frac{1}{R(t)}[|n|[1-\mathrm{sgn}(nn')] - 1]\right\}, \quad (15)$$

where the sgn function equals ± 1 according to the sign of its argument.

Equations (11)–(15) constitute another central result of this work. Equation (11) is the mode-coupling equation of the Saffman-Taylor problem in radial Hele-Shaw cell geometry, when kinetic undercooling effects are properly accounted for. Note that by setting $c = 0$ in Eq. (13), one recovers the usual expressions for λ, F, and G obtained for radial Hele-Shaw flows without kinetic undercooling [14]. It is also worth noticing that the linear dispersion relation (12) coincides with the equivalent expression obtained from the purely linear analysis of the expanding bubble problem with kinetic undercooling, previously performed by Dallaston and McCue [33,34]. The most relevant piece of information that can be extracted from the purely linear calculation is the *stability* behavior of the initially circular fluid interface against small perturbations.

Since the linear aspects of the problem have already been thoroughly discussed in Refs. [33,34], in this work we concentrate our attention on the mode-coupling, nonlinear contributions expressed by the functions $F(n,n')$ and $G(n,n')$ in Eq. (11). An important feature of our second-order perturbative approach is the fact that through the coupling of the appropriate Fourier modes, one is able to extract key analytical information about the *morphology* of the interface (shape of the fingering structures) at the onset of nonlinearities [7,14]. We are particularly interested in understanding how kinetic undercooling influences the mechanisms of finger tip broadening and finger tip splitting under radial and rectangular Hele-Shaw flow circumstances. This legitimate nonlinear issue will be discussed in Sec. III.

III. DISCUSSION

The weakly nonlinear, mode-coupling analysis based on Eq. (11) is quite effective in providing very useful clues about the typical shapes of the emerging fingering structures in Hele-Shaw cell problems, both in rectangular [7] and radial [14] flow geometries. In this section, we examine how kinetic undercooling impacts the morphology of the fingered patterns. Considering the importance of the finger tip-splitting phenomena for Hele-Shaw flows, one interesting point to be investigated is to find out if the fingers would tend to be more wide or narrow when kinetic undercooling takes action. Fortunately, it has been shown in Refs. [7,14] that to do this, one does not need to consider the complicated coupling of an infinite (or a large) number of Fourier modes, but just has to examine the interaction of two specific modes: namely, a fundamental mode and its associated first harmonic. In this way, the basic morphological mechanisms of finger tip broadening, finger tip splitting, or finger tip narrowing could already be efficiently captured at the lowest nonlinear order, and by considering the interplay between just two Fourier modes. This useful approach will be used in Secs. III A and III B below. It should be stressed that the effectiveness of this particular weakly nonlinear strategy has been amply substantiated by a number of analytical, numerical, and experimental studies in the Hele-Shaw flow literature (see, for instance, Refs. [45–53]).

We point out that the theoretical results presented throughout this work are obtained by utilizing parameter values that are consistent with those used in typical experimental realizations of rectangular [1,4,6,8] and radial [9–13] flows in Hele-Shaw cells, as well as with dynamic contact angles studies [37–43].

A. Kinetic undercooling effects: Radial geometry

To examine the shape of the uprising fluid fingering structures at the weakly nonlinear regime under the presence of kinetic undercooling effects in radial geometry, we follow Ref. [14]. We begin our analysis by rewriting Eq. (11) in terms of cosine and sine modes, where the cosine $a_n = \zeta_n + \zeta_{-n}$ and sine $b_n = i(\zeta_n - \zeta_{-n})$ amplitudes are real valued. As in [14], we choose the phase of the fundamental mode so that $a_n > 0$ and $b_n = 0$. As pointed out earlier, within the scope of our mode-coupling description, finger tip broadening and finger tip narrowing can be described by considering the influence of a fun-

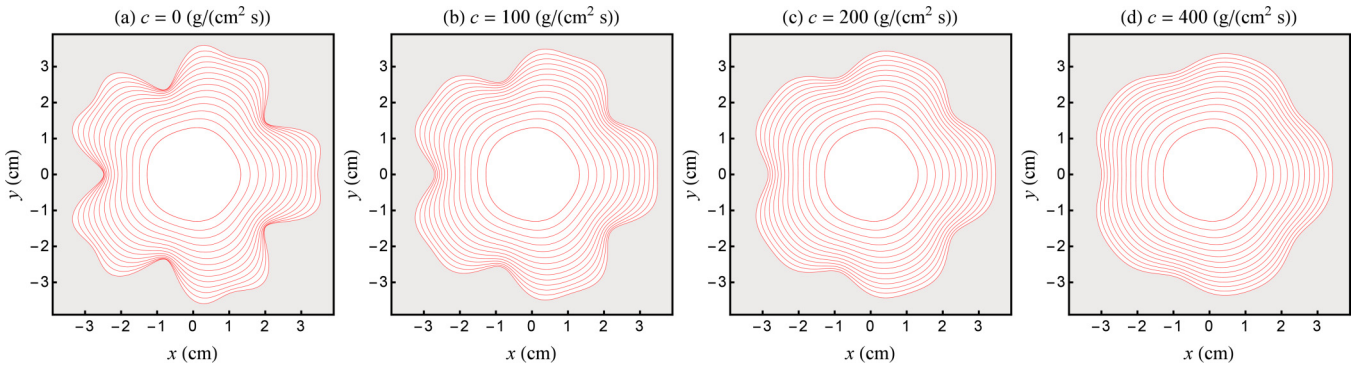

FIG. 1. (Color online) Snapshots of the evolving interface shown at equal time intervals for the interaction of two cosine modes (a_n and a_{2n}, with $n = 5$) for increasingly larger values of the kinetic undercooling parameter c. All of these patterns evolve until the same final time, $t_f = 3.2$ s, with $0 \leqslant t \leqslant t_f$. The region colored in gray represents the more viscous fluid 2.

damental mode n on the growth of its first harmonic $2n$. Writing the equations of motion for the harmonic mode, we have

$$\dot{a}_{2n} = \lambda(2n)a_{2n} + \tfrac{1}{2}T(2n,n)a_n^2, \tag{16}$$

$$\dot{b}_{2n} = \lambda(2n)b_{2n}, \tag{17}$$

where the finger tip function is defined as

$$T(2n,n) = F(2n,n) + \lambda(n)G(2n,n). \tag{18}$$

Since the growth of the sine mode b_{2n} is uninfluenced by a_n and does not present second-order couplings [Eq. (17)], we focus on the growth of the cosine mode a_{2n} which is given by Eq. (16).

Even without explicitly solving Eq. (16), just by inspection one can assess valuable information about possible shapes assumed by the emergent interfacial fingers. It is known that the function $T(2n,n)$ dictates the finger tip behavior [14]. From Eq. (16), notice that depending on the sign of $T(2n,n)$, the term of order a_n^2 can drive the growth of a_{2n} either positively or negatively. If $T(2n,n) < 0$, a_n^2 is driven negatively, making the outward pointing fingers of the inner fluid 1 tend to be wide and flat at their tips. This favors the development of finger tip-splitting events. Reversing the sign of $T(2n,n)$ exactly reverses the above conclusions. If the finger tip function is positive, then a_n^2 is driven positively, a phase that results in narrow outward pointing fingers of fluid 1.

To begin extracting the most relevant morphological features of the emerging fingering patterns by using the weakly nonlinear approach, in Fig. 1 we plot the interface evolution for increasing values of the kinetic undercooling parameter c. All patterns evolve up until the same final time $t_f = 3.2$ s, and we consider the interplay of the fundamental mode $n = 5$ with its first harmonic $2n = 10$. In this plot, we consider that $Q = 3\pi$ cm^2/s, $\eta_1 = 0$, $0.5 \leqslant \eta_2 \leqslant 7$ g/(cm s), $b = 0.15$ cm, $10 \leqslant \sigma \leqslant 60$ dyne/cm, and $R_0 = 1$ cm. The initial amplitudes are $a_n(0) = R_0/100$ and $a_{2n}(0) = 0$. It is important to point out that although in this work we have chosen to use moderate values of the kinetic undercooling parameter [$0 \leqslant c \leqslant 400$ g/(cm^2 s)], in principle it can assume larger values. By utilizing the various possible combinations of experimental data given in Refs. [1,4,6,8–13,37–43], we estimate that c can reach values of the order 10^3 g/(cm^2 s).

From the inspection of Fig. 1, it is clear the kinetic undercooling disfavors finger formation in general and, in particular, restrains the occurrence of finger tip splitting. While in Fig. 1(a) we have sizable fingers that evidently show finger tip splitting, as c is increased in Figs. 1(b)–1(d) these fingers decreased in length, and the finger tip-splitting phenomenon is no longer observed. Even though finger tip-splitting events are not analyzed in Ref. [34], these weakly nonlinear findings are in accordance with their advanced time numerical simulations, where it has been shown that kinetic undercooling delays the formation of fingers.

Nonetheless, from Fig. 1, it is not evident if the emergence of finger tip splitting is either fully suppressed or just delayed by the action of kinetic undercooling. To investigate this relevant issue, in Fig. 2 we use the same physical parameters and the same initial conditions utilized in Fig. 1, but now let the patterns grow up until the largest time ($t = \tau$) for which our weakly nonlinear theoretical results are valid. To determine these values of τ, we follow an approach originally proposed by Gingras and Rácz [54] for the linear regime and extend its range of applicability to the weakly nonlinear stage of evolution. While plotting the evolving interfaces depicted in Fig. 2, we stop the time evolution of the patterns as soon as the base of the fingers starts to move inwards, which would make successive interfaces cross one another. Since this crossing is not observed in experiments [2,9–13], as in Ref. [54] we adopt the largest time before crossing as the upper bound time for the validity of our theoretical description. The usefulness and effectiveness of this criterion has been demonstrated in Ref. [54].

Thus, for our radial injection problem, the instant when the interfacial velocity becomes negative for the first time gives an upper limit for the period in which the weakly nonlinear description is valid. This validity condition can be mathematically expressed as

$$\left[\frac{d\mathcal{R}}{dt}\right]_{t=\tau} = [\dot{R}(t) + \dot{\zeta}(\theta,t)]_{t=\tau} = 0. \tag{19}$$

Notice that differently from what has been done in Ref. [54], we evaluate Eq. (19) by taking into account second-order contributions for interface perturbation $\zeta(\theta,t)$, as prescribed by our mode-coupling equation (11).

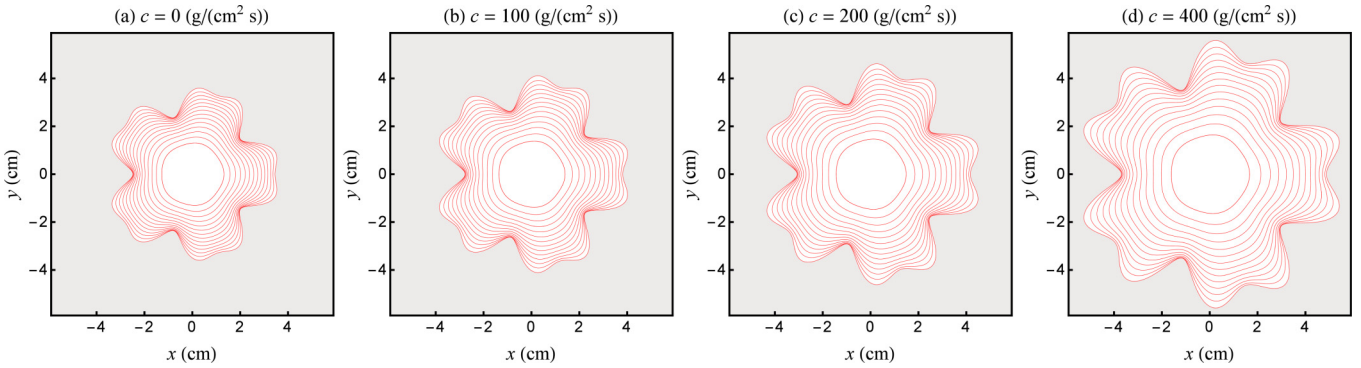

FIG. 2. (Color online) Snapshots of the evolving interface shown at equal time intervals for the interaction of two cosine modes (a_n and a_{2n}, with $n = 5$) for increasingly larger values of the kinetic undercooling parameter c. Differently from Fig. 1, here the patterns evolve until the largest allowed time τ [$0 \leqslant t \leqslant \tau$], computed by Eq. (19): (a) 3.2 s, (b) 4.2 s, (c) 5.3 s, and (d) 7.8 s. Note that Fig. 1(a) is identical to Fig. 2(a). The region colored in gray represents the more viscous fluid 2.

What we observe in Fig. 2 is appreciably different from what we found in Fig. 1: now, despite the fact that c is increasing, we still verify the formation of wide fingers having blunt tips. As a matter of fact, in Figs. 2(a)–2(d), we detect grown fingers that clearly start to bifurcate by splitting at their tips. This happens even for large values of the kinetic undercooling parameter, as illustrated in Fig. 2(d). Actually, tip splitting is most apparent in Fig. 2(d). These findings indicate that kinetic undercooling delays the onset of finger tip splitting, but never fully inhibits it.

We close this section by presenting Fig. 3, which illustrates a parametric plot expressing the behavior of the ratio $a_{2n}(t)/R(t)$ relative to $a_n(t)/R(t)$ as time advances, for the situations depicted in Figs. 1 and 2. The solid curves describe the situations illustrated in Fig. 1 as c is varied, when time runs

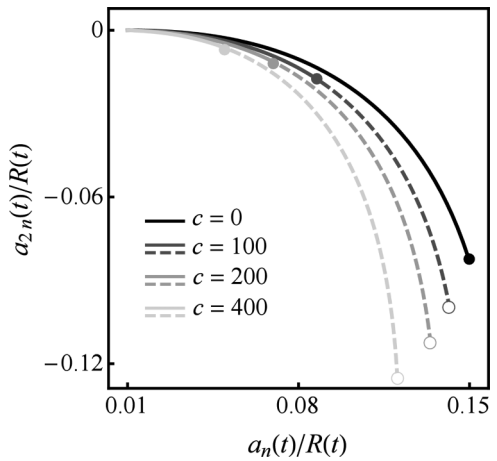

FIG. 3. Behavior of $a_{2n}(t)/R(t)$ with respect to $a_n(t)/R(t)$ in the absence ($c = 0$) and presence ($c \neq 0$) of kinetic undercooling effects, for the pattern evolutions depicted in Figs. 1 and 2. Note that c is given in units of g/(cm^2 s). Solid curves refer to the situations shown in Fig. 1, where $0 \leqslant t \leqslant t_f$, with $t_f = 3.2$ s. The points related to this final time are represented by solid circles. Dashed curves refer to the situations shown in Fig. 2, associated with the time intervals $t_f \leqslant t \leqslant \tau$, where τ is the largest allowed time for each c, as calculated by Eq. (19). For a given value of c, the time $t = \tau$ is indicated by an open circle.

in the interval $0 \leqslant t \leqslant t_f$, where $t_f = 3.2$ s. For each value of c, this time t_f is indicated by a solid circle. On the other hand, the dashed curves are related to the pattern evolutions shown in Fig. 2, and refer to the time interval $t_f \leqslant t \leqslant \tau$. For each value of c, the corresponding value of the largest allowed time τ is represented by an open circle. Of course, when $c = 0$, t_f coincides with τ, and the solid and open back circles overlap so that only the solid black circle is shown in Fig. 3.

The type of graph portrayed in Fig. 3 is convenient to contrast the morphologies for the cases with and without kinetic undercooling, since the ratio $a_n(t)/R(t)$ is related to the average size and overall n-fold symmetry of the patterned structure, while $a_{2n}(t)/R(t)$ determines the typical morphology of the finger tip (i.e., if the tips are wide and split, or if they are narrow and get sharper). By inspecting the solid circles in Fig. 3, we can verify more quantitatively the damping effect of the kinetic undercooling that has been visualized in Fig. 1: for larger values of c, the solid circles indicate smaller magnitudes of both perturbation amplitudes $a_n(t)$ and $a_{2n}(t)$ for the same final time t_f of the evolving fluid-fluid interface. It is also clear that as $a_n(t)/R(t)$ is increased, $a_{2n}(t)/R(t)$ tends to become more and more negative. But, this is precisely the phase of the harmonic that favors finger tip widening and tip splitting. Furthermore, for any given value of $a_n(t)/R(t)$, it is apparent that when $c \neq 0$, the ratio $a_{2n}(t)/R(t)$ is more negative than for $c = 0$. This observation more quantitatively supports our findings extracted from Fig. 2, indicating that kinetic undercooling indeed delays the occurrence of tip-splitting events, but does not keep them from happening.

B. Kinetic undercooling effects: Rectangular geometry

By using the weakly nonlinear equations for the radial flow (12)–(15), we can obtain the corresponding equations for the viscous fingering problem in a rectangular Hele-Shaw cell [7,55]. We will refer to this transformation as the "rectangular geometry limit," which involves the following operations: $R \to \infty$ and $Q \to \infty$ such that $Q/(2\pi R) \equiv v_\infty$ and $n/R \equiv k$ are constant values, where v_∞ is the flow velocity at infinity and k denotes the wave number of the interfacial disturbance. The rectangular geometry limit results in a mode-coupling

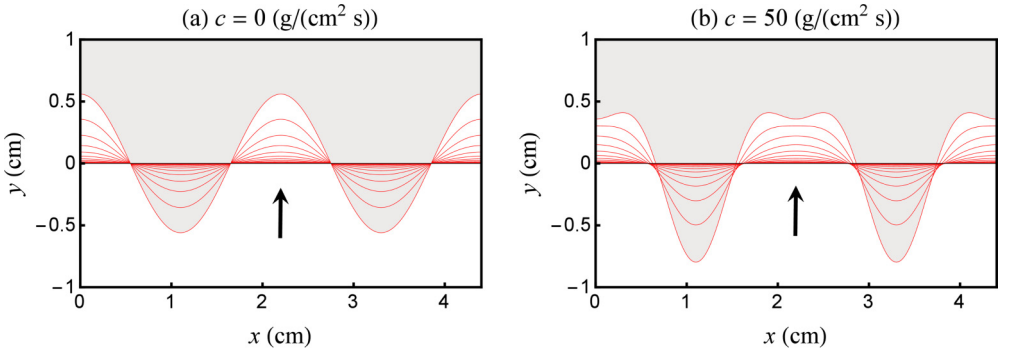

FIG. 4. (Color online) Snapshots of the evolving interface in a rectangular Hele-Shaw cell shown at equal time intervals for the interaction of two cosine modes a_k and a_{2k}, and two values of the kinetic undercooling parameter c: (a) 0 and (b) 50 g/(cm^2 s). The region colored in gray represents the more viscous fluid 2. The vertical arrow represents the direction of the flow velocity.

equation like the one expressed by Eq. (11), where the linear and nonlinear contributions are now given by

$$\lambda(k) = \frac{1}{1+\Theta(k)}|k|(v_\infty - \alpha k^2), \tag{20}$$

$$F\ (k,k') = \frac{\Theta(k)}{1+\Theta(k)}\left[\frac{v_\infty}{2}k'(k'-k)\right], \tag{21}$$

and

$$G(k,k') = \frac{1}{1+\Theta(k)}|k|[1-\mathrm{sgn}(kk')], \tag{22}$$

with

$$\Theta(k) = \frac{cb^2|k|}{12\eta_2}. \tag{23}$$

Notice that the expressions for λ, F, and G are significantly simplified for the rectangular Hele-Shaw flow case. Moreover, in contrast to the corresponding radial flow equations, where the linear and nonlinear functions are time dependent, Eqs. (20)–(23) are constant in time.

In this section, we discuss the role of kinetic undercooling on the development of tip-splitting phenomena in rectangular Hele-Shaw cell geometry. As commented in Sec. I, in contrast to what occurs in radial Hele-Shaw flows, tip-splitting events are not as common in the rectangular cell setup and usually occurs when the flow velocity is sufficiently large [3,6,15–18].

As discussed in Sec. III A, in the framework of our weakly nonlinear analysis, the mechanism of finger tip splitting is connected to the finger tip function (18), which for the rectangular flow case arises from the coupling of the fundamental mode k and its first harmonic $2k$,

$$\dot{a}_{2k} = \lambda(2k)a_{2k} + \tfrac{1}{2}T(2k,k)a_k^2, \tag{24}$$

where

$$T(2k,k) = -\frac{\Theta(2k)}{1+\Theta(2k)}\frac{v_\infty}{2}k^2. \tag{25}$$

Throughout this section, we consider that $k = k^*$ taken when $c = 0$, where k^* is the mode of largest growth rate, obtained by setting $d\lambda(k)/dk = 0$.

One very important aspect of the finger tip function $T(2k,k)$ [Eq. (25)] is that it vanishes in the absence of kinetic undercooling effects. In other words, finger tip splitting [obtained when $T(2k,k) < 0$] would only arise if $c \neq 0$. This fact is clearly illustrated in Fig. 4, which plots the time evolution of the fluid-fluid interface for the case of two interacting cosine modes a_k and a_{2k}. The plot is obtained in such a way that the amplitude of the fundamental mode reaches the value $a_k = 0.6$ cm for both $c = 0$ [Fig. 4(a)] and $c = 50$ g/(cm^2 s) [Fig. 4(b)]. Here we consider that $\eta_1 = 0$, $0.5 \leqslant \eta_2 \leqslant 7$ g/(cm s), $b = 0.15$ cm, $10 \leqslant \sigma \leqslant 60$ dyne/cm, and $v_\infty = 5$ cm/s. The initial amplitudes are $a_k(0) = 1/1000$ cm and $a_{2k}(0) = 0$.

Supplementary information about the tip-splitting behavior in rectangular flows is provided by Fig. 5. It illustrates how the finger tip function $T(2k,k)$ varies with the kinetic undercooling parameter c for three values of v_∞: 2.5 cm/s ($k^* = 2.02$ cm^{-1}), 5.0 cm/s ($k^* = 2.85$ cm^{-1}), and 10 cm/.s ($k^* = 4.04$ cm^{-1}). Since more negative values of $T(2k,k)$ imply an augmented finger splitting, it is obvious that for a given v_∞, the tendency toward tip splitting increases for larger values of c. This is consistent with the equivalent radial flow behavior plotted in Figs. 2 and 3. Finally, in agreement with what has been found in Refs. [3,6,15–18], in Fig. 5 we can also see that tip splitting is favored for larger values of v_∞.

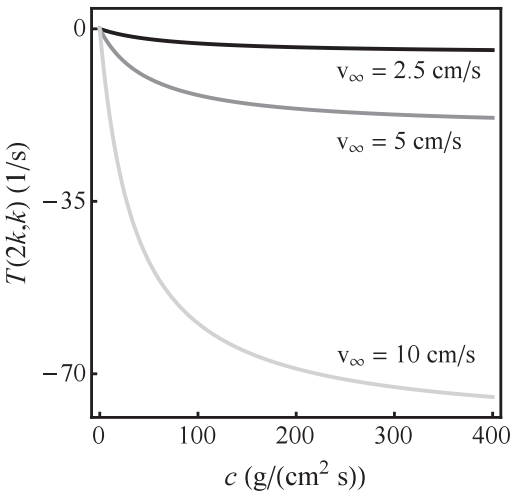

FIG. 5. Variation of the finger tip function $T(2k,k)$ with the kinetic undercooling parameter c, for different values of the velocity v_∞. More negative values of $T(2k,k)$ mean enhanced tip splitting.

IV. CONCLUDING REMARKS

Even though the consideration of kinetic undercooling effects is somewhat common in the research of Stefan-like problems involving melting and freezing, and in the study of streamer discharges, the inclusion of such effects in Hele-Shaw flow problems has been relatively neglected. One of the possible reasons for the insufficient attention given to the influence of kinetic undercooling on the Saffman-Taylor instability is perhaps the fact that this concept was originally introduced in an overly *ad hoc* fashion [30].

In the early 1980s, Romero [30] proposed, without quantitative justification, that a kinetic undercooling-type condition would arise in the Hele-Shaw context if one considered the contribution of the transverse interfacial curvature, and assumed that it was a linear function of the velocity. Then, in 1990, Weinstein *et al.* [31] proposed a dynamic contact angle model, but their asymptotic approach was restricted to steady state circumstances in rectangular Hele-Shaw cells. The problem was recently revisited by Dallaston and collaborators [33–36] who analyzed various interesting aspects connected to the action of kinetic undercooling effects in both radial and rectangular Hele-Shaw geometries. Nevertheless, Dallaston *et al.* did not address the issue of how to incorporate the dynamic contact angle into a general Hele-Shaw flow problem in a more quantitative manner.

Considering the current state of affairs regarding the topic of kinetic undercooling in Hele-Shaw flows, this work tackles two main issues: first, we show, by using the Hoffman-Voinov-Tanner law, that the consideration of the dynamic contact angle effects does lead to a kinetic undercooling condition which varies linearly with the normal velocity on the interface. As a byproduct, our approach allows one to relate the kinetic undercooling parameter c to other key physical properties of the problem. A second important point was acquiring a basic understanding of how kinetic undercooling impacts pattern formation processes in the the Saffman-Taylor problem, both in radial and in rectangular flow setups. Our weakly nonlinear results indicate that in radial cells, kinetic undercooling tends to delay (without entirely suppressing) the occurrence of finger tip-splitting events. This result is in line with the numerical simulation findings of Dallaston and McCue [34]. Moreover, we have found analytically that kinetic undercooling favors the emergence of tip-splitting phenomena in rectangular cells, if the interface velocity is sufficiently high. This last result is consonant with what has been previously obtained by numerical [3,15,16] and experimental [6,17,18] studies on this particular rectangular flow issue.

We hope that our present study will motivate researchers to further study this rich and still poorly explored topic of kinetic undercooling effects in Hele-Shaw flows.

ACKNOWLEDGMENTS

J.A.M. and P.H.A.A. thank CNPq and FACEPE (through PRONEM Project No. APQ-1415-1.05/10) for financial support. E.O.D. acknowledges financial support from FACEPE through PPP Project No. APQ-0800-1.05/14.

[1] P. G. Saffman and G. I. Taylor, Proc. R. Soc. London A **245**, 312 (1958).
[2] For review articles on this subject, see, for instance, D. Bensimon, L. P. Kadanoff, S. Liang, B. I. Shraiman, and C. Tang, Rev. Mod. Phys. **58**, 977 (1986); G. M. Homsy, Annu. Rev. Fluid Mech. **19**, 271 (1987); K. V. McCloud and J. V. Maher, Phys. Rep. **260**, 139 (1995); J. Casademunt, Chaos **14**, 809 (2004).
[3] A. J. DeGregoria and L. W. Schwartz, J. Fluid Mech. **164**, 383 (1986).
[4] C.-W. Park and G. M. Homsy, J. Fluid Mech. **139**, 291 (1984).
[5] P. G. Saffman, J. Fluid Mech. **173**, 73 (1986).
[6] T. Maxworthy, J. Fluid Mech. **177**, 207 (1987).
[7] J. A. Miranda and M. Widom, Int. J. Mod. Phys. B **12**, 931 (1998).
[8] C. Chevalier, M. Ben Amar, D. Bonn, and A. Lindner, J. Fluid Mech. **552**, 83 (2006).
[9] L. Paterson, J. Fluid Mech. **113**, 513 (1981).
[10] H. Thomé, M. Rabaud, V. Hakim, and Y. Couder, Phys. Fluids A **1**, 224 (1989).
[11] J.-D. Chen, J. Fluid Mech. **201**, 223 (1989); Exp. Fluids **5**, 363 (1987).
[12] S. S. S. Cardoso and A. W. Woods, J. Fluid Mech. **289**, 351 (1995).
[13] O. Praud and H. L. Swinney, Phys. Rev. E **72**, 011406 (2005).
[14] J. A. Miranda and M. Widom, Physica D **120**, 315 (1998).
[15] S. D. Howison, J. Fluid Mech. **167**, 439 (1986).
[16] E. Meiburg and G. M. Homsy, Phys. Fluids **31**, 429 (1988).
[17] P. Tabeling, G. Zocchi, and A. Libchaber, J. Fluid Mech. **177**, 67 (1987).
[18] A. Arnéodo, Y. Couder, G. Grasseau, V. Hakim, and M. Rabaud, Phys. Rev. Lett. **63**, 984 (1989).
[19] W. S. Dai, L. P. Kadanoff, and S. M. Zhou, Phys. Rev. A **43**, 6672 (1991).
[20] M. Siegel and S. Tanveer, Phys. Rev. Lett. **76**, 419 (1996).
[21] J. Casademunt and F. X. Magdaleno, Phys. Rep. **337**, 1 (2000).
[22] J. R. King and J. D. Evans, SIAM J. Appl. Math. **65**, 1677 (2005).
[23] S. Chen, B. Merriman, S. Osher, and P. Smereka, J. Comp. Physiol. **135**, 8 (1997).
[24] J. M. Back, S. W. McCue, and T. J. Moroney, Appl. Math. Comp. **229**, 41 (2014).
[25] J. M. Back, S. W. McCue, and T. J. Moroney, Sci. Rep. **4**, 7066 (2014).
[26] C. Misbah, H. Müller-Khumbhaar, and D. E. Temkin, J. Phys. I (France) **1**, 585 (1991).
[27] F. Gibou, R. Fedkiw, R. Caflisch, and S. Osher, J. Sci. Comput. **19**, 183 (2003).
[28] B. Meulenbroek, U. Ebert, and L. Schäfer, Phys. Rev. Lett. **95**, 195004 (2005).
[29] F. Brau, A. Luque, B. Meulenbroek, U. Ebert, and L. Schäfer, Phys. Rev. E **77**, 026219 (2008).

[30] L. A. Romero, Ph.D. thesis, California Institute of Technology, 1981.
[31] S. J. Weinstein, E. B. Dussan V., and L. H. Ungar, J. Fluid Mech. **221**, 53 (1990).
[32] H.-W. Lu, K. Glasner, A. L. Bertozzi, and C.-J. Kim, J. Fluid Mech. **590**, 411 (2007).
[33] M. C. Dallaston and S. W. McCue, Nonlinearity **26**, 1639 (2013).
[34] M. C. Dallaston and S. W. McCue, ANZIAM J. **54**, C309 (2013).
[35] M. C. Dallaston and S. W. McCue, Eur. J. Appl. Math. **25**, 707 (2014).
[36] B. P. J. Gardiner, S. W. McCue, M. C. Dallaston, and T. J. Moroney, Phys. Rev. E **91**, 023016 (2015).
[37] R. L. Hoffman, J. Colloid. Interface Sci. **50**, 228 (1975).
[38] O. V. Voinov, Fluid Dyn. **11**, 714 (1976).
[39] L. H. Tanner, J. Phys. D **12**, 1473 (1979).
[40] R. G. Cox, J. Fluid Mech. **168**, 169 (1986).
[41] T. D. Blake, J. Colloid. Interface Sci. **299**, 1 (2006).
[42] D. Bonn, J. Eggers, J. Indekeu, J. Meunier, and E. Rolley, Rev. Mod. Phys. **81**, 739 (2009).
[43] E. Alvarez-Lacalle, J. Ortín, and J. Casademunt, Phys. Rev. E **74**, 025302(R) (2006).
[44] P. Sheng and M. Zhou, Phys. Rev. A **45**, 5694 (1992).
[45] E. Alvarez-Lacalle, E. Pauné, J. Casademunt, and J. Ortín, Phys. Rev. E **68**, 026308 (2003).
[46] E. Alvarez-Lacalle, J. Ortín, and J. Casademunt, Phys. Fluids **16**, 908 (2004).
[47] H. Gadêlha and J. A. Miranda, Phys. Rev. E **70**, 066308 (2004).
[48] A. Lindner, D. Derks, and M. J. Shelley, Phys. Fluids **17**, 072107 (2005).
[49] J. A. Miranda and E. Alvarez-Lacalle, Phys. Rev. E **72**, 026306 (2005).
[50] C.-Y. Chen, C.-H. Chen, and J. A. Miranda, Phys. Rev. E **73**, 046306 (2006).
[51] R. Folch, E. Alvarez-Lacalle, J. Ortín, and J. Casademunt, Phys. Rev. E **80**, 056305 (2009).
[52] R. Brandão, J. V. Fontana, and J. A. Miranda, Phys. Rev. E **90**, 053003 (2014).
[53] P. H. A. Anjos and J. A. Miranda, Soft Matter **10**, 7459 (2014).
[54] M. J. P. Gringras and Z. Rácz, Phys. Rev. A **40**, 5960 (1989).
[55] For more information about the treatment of Saffman-Taylor fingers in a rectangular Hele-Shaw cell with kinetic undercooling, see, for instance, S. J. Chapman and J. R. King, J. Eng. Math. **46**, 1 (2003).